A Two-Dimensional Model for the Free-Settling Regime in Continuous Thickening

All classical models for thickening assume one-dimensional continuity. However, the free-settling domain in continuous thickeners is not one-dimensional. Therefore, a two-dimensional model is investigated. The two-dimensional model gives the same values for thickener area demands as the one-dimensional model, but the relationships between batch and steady-state thickening are not the same. Free-settling Kynch characteristics can arise in the continuous operation that do not arise in batch tests. Therefore, design procedures that rely on Kynch theory, such as that of Talmage and Fitch, are not completely valid.

A method is developed, based on extrapolating the Kynch or free-settling segment of a batch settling curve, that yields an improved prediction for thickener area demand.

Bryant Fitch
1570 Oak St.
Napa, CA 94559

Introduction

All classical flux models for thickening assume one-dimensional continuity. This is reasonable for batch settling in cylindrical columns, except perhaps where channeling occurs. The free-settling domain in operating thickeners, however, is not one-dimensional. New feed suspension, which contains settleable solids and therefore is denser than the supernatant, plunges as a "submerged waterfall" to its level of hydrostatic equilibrium. There it spreads out horizontally as a "density current," either just above the compression zone or above a critical zone if one exists (Figure 1). While it is spreading out, solids pass directly into the subjacent zone together with that part of the liquid destined for the underflow. Therefore, some justification is needed for the application of one-dimensional continuity equations to the two-dimensional flow.

While suspension is spreading out in the feed layer zones of constant concentration will be propagating upward through it much as they do in batch tests. We do not know how thick the feed layer is at any point, nor do we know the velocity profiles in it. Suspension at one level may be moving laterally at different rates than at other levels. Unless these things are known, we cannot predict where the characteristics are located or what the concentration will be at any given point in the zone. Fortunately, for engineering purposes there is no need to know.

The Area Principle

In the extensive literature on settling basins, sedimentation has always been treated as two-dimensional, and the two-dimensional nature of the free-settling domain in thickening was observed by Turner and Glasser (1976). Hazen (1906) showed that for an "ideal" two-dimensional settling basin the amount of solids settling out depends only on the overflow flux (volume overflowing/basin area) and the settling rate of the solids. It is independent of basin depth. This was generalized (Fitch, 1956) to show that it remained valid even for nonideal basins, in which local velocity vectors varied in direction and magnitude along the flow paths. In the following it will be shown that the same principle applies for the amount of solids passing through a Kynch characteristic.

Generalized proof of area principle

A general proof of the area principle for characteristics is now given:

The time dt needed for an element of flow dQ to pass through an element of space bounded by flow lines is shown in Figure 2:

$$dt = (dH)(dW)(dy)/dQ \tag{1}$$

However, since $(dW)(dy) = dA$

$$dt = (dH)(dA)/dQ \tag{2}$$

The time it takes a characteristic surface to rise from the bottom to the top of the flow element is:

$$dt = (dH)/v_K \tag{3}$$

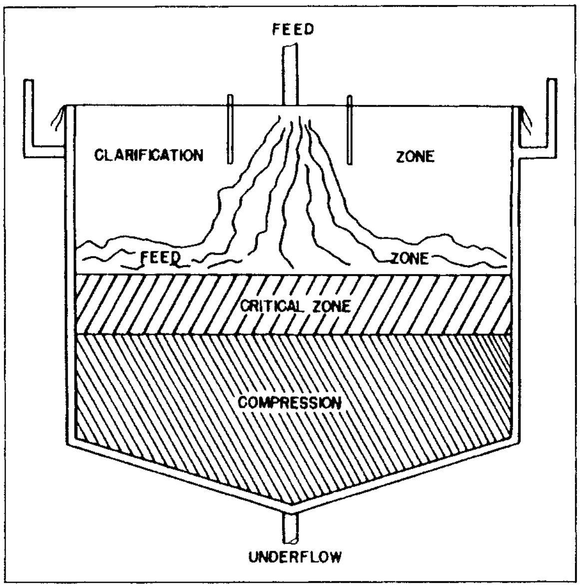

Figure 1. Thickener flow patterns, overloaded operation.

Equating the two:

$$dA = dQ/v_K \tag{4}$$

Integrating over all area elements traversed by the characteristic surface:

$$A_{ch} = Q/v_K \tag{5}$$

where A_{ch} is the area at which the characteristic plane reaches the pulp-supernatant interface and disappears, just as Kynch characteristics disappear when they reach the interface in a batch test.

From the derivation of Eq. 5, it follows that it will be valid regardless of the magnitude, direction and divergence of the flow vectors. In particular it will be valid for the usual centrally-fed circular basin.

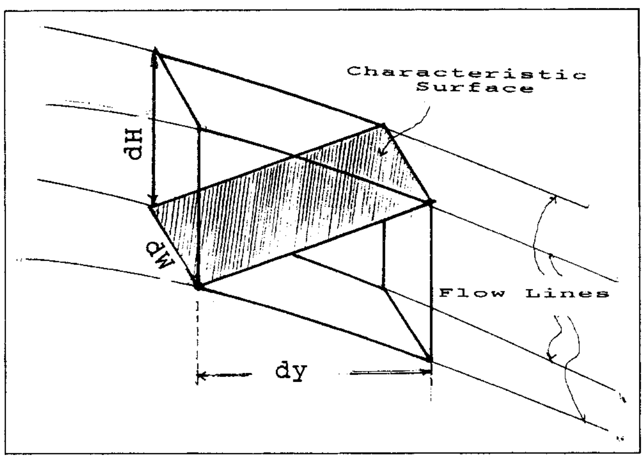

Figure 2. Differential space element crossed by a characteristic surface.

Thickener Operation

In direct violation of one-dimensional continuity, every characteristic concentration that can arise is present in the feed zone of a thickener, to whatever area is given for the concentration in question by Eq. 5. Beyond this area, all the solids present will be in characteristics of higher concentration.

In the feed zone, the solids settle directly into a subjacent region in which the flow is, in effect, one-dimensional. In normal operation, this will be a compression zone, but if the thickener is overloaded it may be a critical free-settling one.

In an underloaded thickener, all the solids will have settled into the subjacent compression zone before the flow reaches the periphery or discharge end of the thickener. However, although there are no solids settling into the compression zone at greater distances from the feed point, the boundary between the feed zone and the compression zone remains in fact essentially level. Solids at the top of the compression zone obviously slump to fill the full thickener area. Therefore, the transport velocity v_u is determined by the full thickener area A_t, rather than by that of the limiting characteristic A_{ch}.

In an overloaded thickener, all the solids will not have entered the compression zone by the time the feed flow reaches the discharge. Since they cannot settle into the compression zone, they will build up as a "critical zone" above the compression one until the critical zone fills the thickener. The feed zone then runs across the thickener at overflow level. Any solids that cannot settle into and through the critical zone will spill out with the supernatant when it reaches discharge. The concentration in such a critical zone will be that of the characteristic whose net upward propagation rate is zero. Any with a negative net upward propagation rate would not emerge from the boundary between compressing pulp and the critical suspension above it. Any with a positive net upward propagation rate would have immediately risen above the level of the compression-suspension interface and could not be superjacent to it.

Cross-Flow Model

The area principle shows that the area demands remain the same regardless of the lateral velocity components, inclinations and divergences of the suspension in the free-settling region. Therefore, if the area demands can be calculated for any one suspension flow pattern, they would be valid for any other. Accordingly, batch settling results will be related to the area demands of a highly idealized thickener, which will in turn be identical to those of a corresponding nonideal one. This makes no assumptions whatsoever about the actual flow pattern in the nonideal thickener, except that it is uniformly distributed. That is, the velocity components and concentration profiles are the same at any given distance along the flow paths from the feed source.

The idealized model, Figure 3, is assumed to be rectangular in plan, with two-dimensional flow across a feed zone. Flow velocity vectors in the feed zone are assumed the same everywhere. The bottom of the feed zone is defined by an interface with a subjacent compression zone. Initially no assumptions will be made about flow in the compression zone, except that the boundary between this and the feed zone remains level.

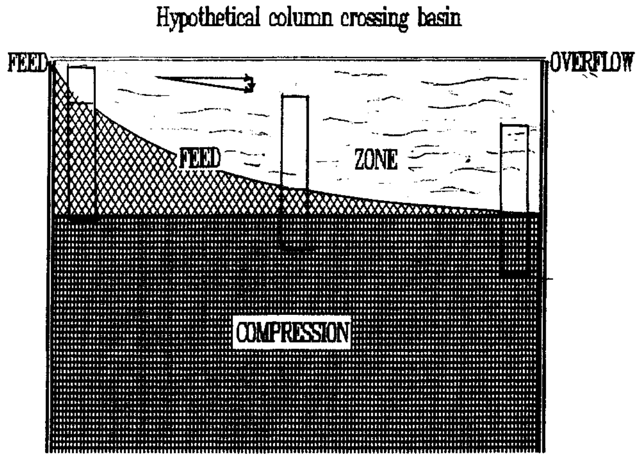

Figure 3. Idealized crossflow thickener model.

At all levels in the thickener, the settling system has a transport velocity v_u as a result of underflow withdrawal where:

$$v_u = Q_u/A = Q_s/(Ac_u) \quad (6)$$

Therefore, the flow velocity vectors in the cross-flow model will have a downward component equal to v_u.

Relationships between batch and continuous thickening

A column of suspension is identified at the feed end of the cross-flow zone. What happens within the marked column as it follows the flow across the basin is closely analogous to what happens in a batch settling test. The difference is that in a batch column the suspension as a whole does not move downward, and a compression region builds up from the bottom of the column. The two can be compared directly by transforming the moving column to a coordinate system moving downward at a velocity equal to the downward transport velocity v_u. In this new coordinate system, Kynch characteristics would propagate upward at exactly the same rate as those in the batch test. However, in this coordinate system the bottom of the hypothetical moving column would sink down past the interface between the free-settling and compression zones. Thus the compression pulp would be displaced up into the column at a constant rate $-v_u$. In this hypothetical batch column the L curve, marking the bottom of the free settling suspension, would be linear. As far as material balance across the L surface and the behavior of the superjacent free-settling region are concerned, it is as though the solids settle batchwise into a noncompressing zone of concentration c_u, even though the solids actually are compressed in the zone below.

There would be no difference between the true batch settling and this hypothetical cross-flow column if the solids were incompressible (as envisaged by Kynch, 1952). The L curve would be the same for both the batch and the cross-flow columns. However, where the solids are compressible the solids do not collapse directly into an underflow concentration c_u. They have to be compressed to it. Therefore, the average concentration beneath the L curve is lower than c_u in the batch case. The volume of solids in the sediment at any time is greater, and the L curve rises faster than in the incompressible case. As shown in Figure 4, the line connecting a to d is the experimental batch settling plot, and Line 0–c is the L curve showing rise of the sediment-supernatant interface. Line a–b–c′–d′ is the hypothetical settling plot, and 0–c′ is the hypothetical L curve.

The characteristic that is limiting for continuous thickening would have a propagation rate equal to v_u. It would not emerge in a batch test in which solids are compressible. The compression discontinuity rises faster. The theoretical locus of the critical characteristic would be everywhere overrun by the rising compression zone. Since the critical concentration does not emerge, its flux-handling capacity or area demands cannot be deduced directly by Kynch constructions. The Talmage and Fitch (1955) method for determining area demands from a single-batch settling test is therefore not theoretically valid.

Unit Areas by Extrapolation

A value for area demand can, however, be estimated by extrapolation of the free-settling part of a batch settling curve.

If it were not for the existence of a compression zone and solids could collapse directly from free settling to underflow concentration, then Kynch characteristics of all concentrations up to that whose propagation rate was equal to $-v_u$ could arise in a batch test. The free-settling range of a batch settling curve would not then be terminated until underflow concentration had propagated to the suspension-supernatant interface. That part of the hypothetical settling curve beyond the compression point in a real test would simply be an extrapolation of the free-settling part of the real curve. Kynch theory could be applied to the extrapolated region, and the free-settling characteristics that do not arise in a batch test could be simulated. The problems are first to properly extrapolate the free-settling part of the curve and then to interpret the resulting hypothetical curve.

Extrapolation of the free-settling curve relies on the assumption that the permeability of the solids considered as a porous medium is a well-behaved function of solids concentration and hence can be extrapolated. That is, if the function can be determined from the free-settling part of a curve, it will remain

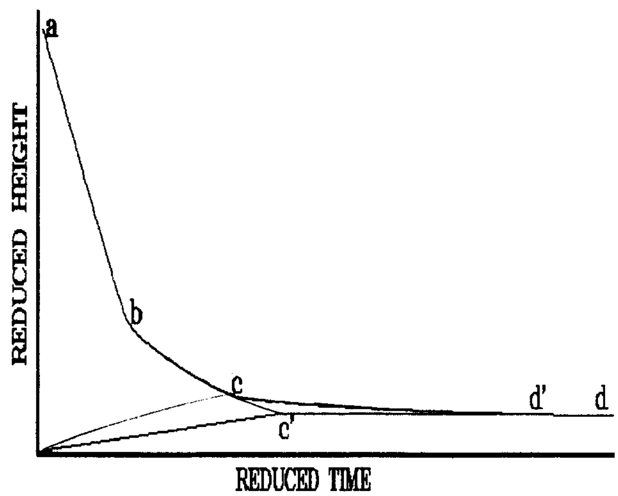

Figure 4. Settling plot showing actual and extrapolated free-settling domains.

valid for the extrapolated part also. However, the analyses to follow will extrapolate on the basis of free-settling rates and settling flux S. Therefore, it is more convenient to work with the variable u^*, defined as settling rate in the absence of solids pressure gradients or, in other words, the free-settling rate. This is related to permeability K as will be explained next.

Relation of u^* to permeability K

First, it should be noted again that settling rates are here defined as particle velocities in a coordinate system, for which the total volumetric flux (solids + liquid) is zero, i.e., in batch settling coordinates. It is not the same as solids velocity pass an observer in any other system. Free-settling velocity u^* is equal to $-\phi_D$, and the flux in the standard Darcy equation $\phi_D = -(dP_L/dx)K/\mu$. This equivalence can be deduced logically by transforming mentally to a coordinate system in which solids are stationary. The total flux (solids + liquid) would then be equal to $-u^*$; and since in this system the solids are stationary, the total flux would have to be that of the fluid passing the solids or ϕ_D.

From the force balance, neglecting inertial effects and solid stress gradients:

$$g(\rho_s - \rho_f)c = \delta P_L/\delta x$$

From Darcy's law, again neglecting inertial effects:

$$\delta P_L/\delta x = -\phi_D\mu/K = u^*\mu/K$$

Therefore:

$$u^* = Kg(\rho_s - \rho_f)/\mu$$

Extrapolation Procedure

To extrapolate the Kynch section of a settling curve, an empirical function must be found relating these variables through the Kynch range. This will require close delineation of the curve, so a great many data points will be needed, and not many suitable data have been published. However, Tory's thesis (1961) is an exception. It gives a wealth of eminently suitable data. His batch settling tests were made in 6 in. (152 mm) diameter columns, with initial heights up to 1.47 m, and literally hundreds of data points were recorded in most of them. Furthermore, several tests were made with the same initial concentrations, but with different initial heights. This permits testing the validity of the extrapolations, as will be discussed later.

The line a–b–c–d in Figure 4 is a batch settling plot of H vs. time for the Tory's test No. 27. The curve displayed appears superficially much as might be expected from classical flux theories, with an initial constant rate period, followed by a first falling rate or Kynch zone segment, and then a second decreasing rate or compression one. More careful analysis, as described below, reveals significant differences.

Settling plot analysis

Much more detail is revealed in a plot of settling rate R, which is $-dH/dt$, vs. suspension height H. Such plots were introduced by Tory in his thesis, and they will be referred to as "Tory plots."

Slopes dH/dt can be (and originally were) determined from the settling plot data by first choosing an intercept point H_i on the H axis, and then drawing a tangent from it to the field of points. That is, a chord is drawn from it to whichever of the points in the curve gives the steepest slope. The slope of the chord and the height of its terminal point on the settling curve give corresponding values of R and H for a Tory plot. By taking a series of closely-spaced intercept values, data for a Tory plot can be developed. This method has the drawback of developing only an envelope of values. It skips over sections of a settling curve that are concave below, showing them as regions over which subsidence rate remains constant over a range of heights H. Also it does not average out local noise or experimental errors in the settling data. However, local deviations in data points will not result in large errors in the slope of the chords (except at low times) as could be expected when trying to construct tangents to the field of points locally, and smoothing of the data can take place in the Tory plot constructed from the data developed. The method has the advantages of being good at finding slope discontinuities and is well adapted for computer solution. However, it is slow. An algorithm mathematically equivalent, but orders of magnitude faster, is now used and is embodied in computer programs (Fitch, 1990).

Figure 5 shows a Tory plot developed from the data of Figure 4. The height values have been reduced (divided by C_0H_0), which would make all plots coincide where the Kynch assumptions are valid.

In Figure 5 there appear to be several identifiable ranges, all of falling rate. In the final one, corresponding to the range from a to c, the pulp is almost assuredly in compression. This will accordingly be designated as the compression or C range. It, however, may be divided into two subranges. From a to b the plot is linear, as would be expected from the empirical Roberts equation (Roberts, 1949)

$$t = B \ln (H - H_\infty) \tag{7}$$

From Eq. 7 if follows that:

$$-dH/dt = M(H - H_\infty) = R \tag{8}$$

which is linear on a Tory plot.

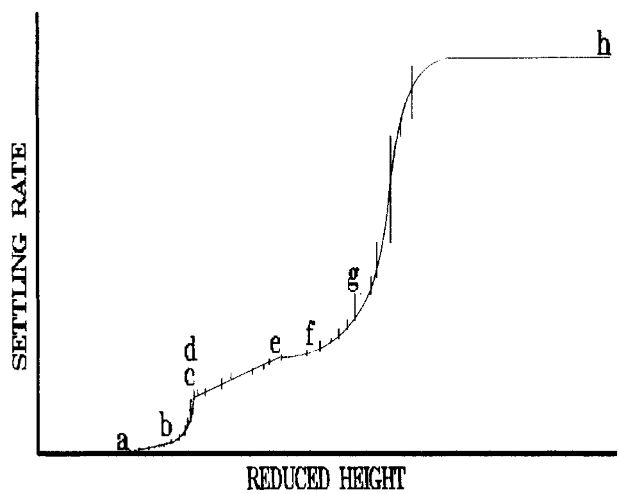

Figure 5. Tory plot for Tory run 27.

Between b and c, there seems to be a transition section, through which the plot is not linear. It might be surmised that through this subrange subsidence rate is being augmented by channeling. In any case, the assumption that b marks the compression point, as has been suggested occasionally by some researchers (including the writer), is clearly untenable.

The next range corresponds to that between points d and g. Through this range, all the plots entering come reasonably close to coinciding. Therefore, in this range Kynch theory should be at least approximately valid. It will accordingly be designated as the Kynch or K range. The K range, however, again appears to comprise two subranges d to e and e to g. The first of these appears to be linear and will be designated as K_1. The second subrange will be designated as K_2.

From g to h there is an initial or I range. It corresponds to the "constant rate section" of classical and Kynch theories, but experimentally is not one of constant rate clearly.

At this time, only the K_1 segment will be considered. Since it is strikingly linear, it can be well represented by:

$$R = M(H - I) \tag{9}$$

Since $R = -dH/dt$, integration yields:

$$t = E - (1/M)\ln(H - I) \tag{10}$$

To the extent that permeability may be assumed to be a well-behaved function of concentration c, each of these equations can be extrapolated to the lower heights and higher times beyond the batch compression point c.

Validity of Extrapolation

The proposed extrapolation would not be valid if there were a change in sedimentation mechanism, as for example the incidence of short-circuiting or channeling. However, its validity for small extrapolations may be tested empirically as follows.

When the characteristics greater than initial concentration arise in a batch test, the rate at which the compression zone builds up is independent of the initial concentration or depth. It is controlled by the concentration of the free-settling characteristic directly superjacent to the compression zone at any time. At any time the superjacent characteristic will have a propagation rate equal to that of the suspension-sediment interface L. Any characteristic with a lower upward propagation rate could not emerge from the boundary layer at the interface; and any with a higher upward propagation rate would have emerged sooner and would no longer be superjacent (since for compressible pulps, the L curve is convex on the top). The total time needed for the compression zone to emerge at the supernatant interface then depends on the total amount of solids present in the test. The compression zone build-up will therefore be the same for all the tests having the same amount of solids. Their reduced batch settling plots should coincide not only through the Kynch region, but also through the compression section. The same would be true for reduced settling plots and for Tory plots.

When the solids are compressible, the L curve is convex above. As the compression zone builds up, the slope of the L curve decreases and therefore also the propagation velocity of the superjacent Kynch characteristic. Thus the more the compression zone builds up, the more Kynch characteristics arise. When there are more solids per unit area present in a test, the compression zone ultimately builds up further. Therefore free-settling characteristics of higher concentration and hence lower upward propagation rates are formed and propagated to the surface. In reduced coordinates, the free-settling section of the settling plot should then be longer, and the compression section should run below that of the tests with less solids. The same should be true for reduced Tory plots.

This is demonstrated in Figures 6A and 6B. They compare in reduced coordinates two of Tory's tests made with different amounts of solids (same initial concentration c_0 but different values of H_0). As expected, the plots coincide through the Kynch segments of the free-settling sections. That is not the case through the compression segments. However, the free-settling leg is longer for the test with the higher solids. What is important is that the K_1 segment of the Tory plot remains linear in both cases. The extra length of the high solids curve is just an extrapolation of what went before and of the corresponding curve for the lower solids case. At least in this case and to the extent tested, extrapolation of the free-settling part of a curve is empirically justified.

The point at which the two curves diverge marks the compression point for the lower solids plot. Note that it falls at a substantially lower time than would be given by conventional empirical procedures. This could account for much of the overdesign noted in applying the Talmage and Fitch procedure.

A more general confirmation of the sedimentation pattern is provided by Figure 7. In it Tory plots for a number of Tory runs are superimposed. The runs were made with three different values of C_0H_0 so that they show three different compression sections. It turns out that settling rates are everywhere greater for the tests in which the initial concentration is greater. Furthermore, duplicate tests show considerable variation. However, Tory plots for all tests show the same general pattern, and the same linearity in the K_1 range.

Design Procedures

There is at present no theoretically sound and empirically confirmed procedure for designing thickeners. All currently used mathematical models have theoretical shortcomings, and

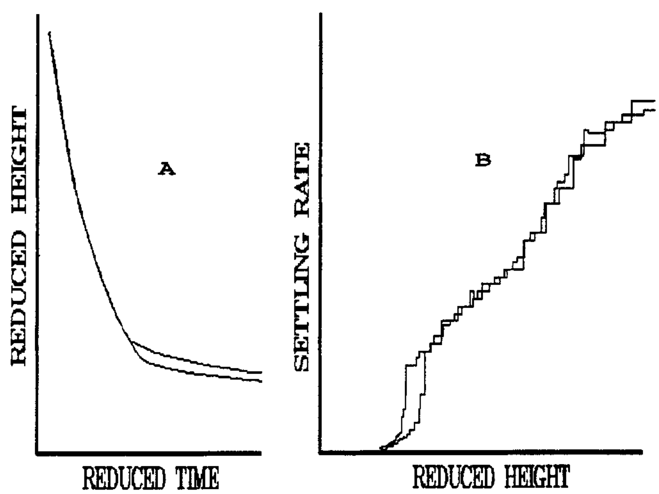

Figure 6. Reduced settling and Tory plots for runs with the same initial concentration, but different initial heights.

Figure 7. Tory plots for a number of tests.

empirically the behavior of thickening suspensions deviates widely from that predicted by the models. However, practicing engineers still have to design thickeners.

The greatest uncertainty arises from short-circuiting. It augments subsidence rates through just the range in which critical concentrations might be predicted from the models. It does so by an unknown and empirically varying amount. At this time there is no procedure for evaluating short-circuiting. All existing design methods implicitly make one assumption or another, which is applied indiscriminately to any and all suspensions.

Based on a very small number of observations, Coe and Clevenger concluded that short-circuiting or channeling would always occur in the compression zone and that it would be there to augment settling rates sufficiently so that critical zones would never occur in compression. They also tacitly concluded that short-circuiting would not occur in free-settling. These assumptions are the classical ones retained to this day in most design procedures. However, experimental evidence has accumulated over the years to indicate that neither of them is necessarily valid (Fitch, 1972).

In the following, procedures will be described for estimating area demands based on the extrapolated free-settling plot such as that shown in Figure 4. In it, the effects of compression and the compression zone have been removed by calculation. That is, a settling plot is synthesized for a hypothetical suspension, in which the Darcian permeability is the same function of concentration as in the prototype suspension, but in which the solids are not compressible. As will be discussed, compressibility of the floc structure does not enter into area demand. Therefore, the area demand determined for this hypothetical suspension will be the same as that for the prototype.

In principle, any method could be used for extrapolation of the free-settling regime. However, experimental evidence shows that the K_1 range in a Tory plot is linear, Eq. 9. Therefore, a Tory plot is made from the batch settling data, and the linear K_1 range is identified. The parameters of the best line through this range are identified, and the corresponding equation for the part of the settling plot to be extrapolated is determined, Eq. 10.

In practice, a computer program (mentioned above) calculates and displays the Tory plot. The user moves marker lines on the plot to delineate the bounds of the linear region, Figure 8. The computer then calculates and displays a least-squares line through the delineated region. It also calculates the parameters for Eq. 10.

The limiting flux G_{max} is now determined by the algebraic equivalent of a Talmage and Fitch construction on a plot defined by Eq. 10. First, an underflow height H_u is arbitrarily specified. It is equal to C_0H_0/c_u and must be one attainable by thickening. Often it will be the lowest height at which a reading was taken. In the computer program, the desired underflow height H_u is selected by a moveable marker on the plot.

At this point, some judgment will have to be made about short-circuiting. Two limiting cases of short-circuiting will be considered: 1. that it is assumed negligible; and 2. that it dominates above the critical concentration.

Case 1: short-circuiting assumed negligible

In the first case, short-circuiting will be considered absent or negligible. In that case, the most limiting flux is that of the characteristic which would surface in the hypothetical test at H_u. The value of time t_u at H_u is then calculated from Eq. 10. From the Talmage and Fitch construction, the maximum solids flux possible through the thickener is then:

$$G_{max} = c_0 H_0 / t_u \tag{11}$$

Case 2: short-circuiting dominates above a critical concentration

In this case, short-circuiting will be assumed to start at some critical concentration c_c and, above this concentration, to augment settling rates sufficiently so that no concentration above it will be limiting. Experimental evidence, which will be discussed subsequently, suggests that often such is the case. This leaves c_c as the limiting concentration, and the one whose hypothetical characteristic determines G_{max}. In this case, the critical height H_c will have to be specified by the engineer on the basis of evidence and judgment. This will be discussed later. In this case, again from the Talmage and Fitch construction:

$$t_u = t_c + u^*(H_c - H_u) \tag{12}$$

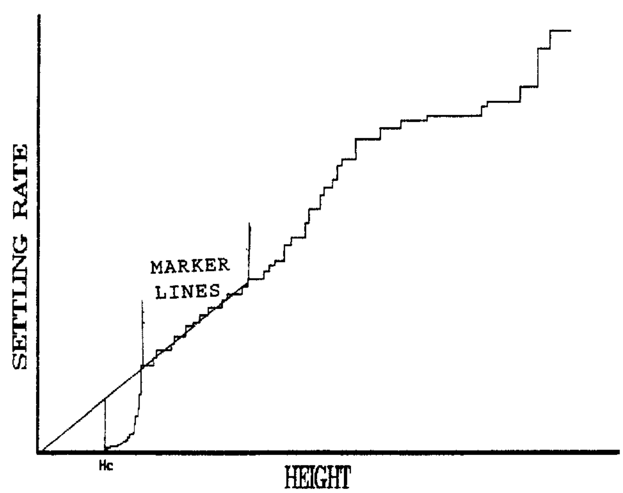

Figure 8. Computer constructions.

And as before

$$G_{max} = c_0 H_0 / t_u \tag{13}$$

We do not at this time have any way of treating intermediate cases, if they exist.

The J-Error

Kynch theory assumes that the solids are incompressible. In that case, the L curve, showing the build-up of the compression zone, is linear. All the characteristics of higher than initial concentration therefore propagate from the origin, and Kynch theory depends on this for determining their concentration. In nearly all applications of thickening, however, the solids are compressible. As discussed earlier, the L curve in that case is not linear. There are high concentration characteristics that arise not from the origin, but tangentially from the L curve. Accordingly, the Kynch construction for determining their concentrations and derivatively the Talmage and Fitch procedure for determining unit areas are not theoretically valid.

A procedure for correcting Kynch theory to account for compression and for determining G_{max} is outlined in the following. It will be of more theoretical than practical interest, since the corrected method requires sophisticated experimental procedures and the error from the uncorrected method can be made small enough to overlook, given all the other uncertainties involved.

As shown in an earlier paper (Fitch, 1983), the concentration of characteristics arising from the L curve can in theory be determined by the construction of Figure 9 (or its analytic equivalent), which provides the measurement of the build-up of the compression zone as well as the subsidence of the pulp-supernatant interface. A tangent is drawn to the settling plot at some point (point a). It intersects the H axis at H_i, and the time axis at t_i. Another line is drawn from point a tangent to the L curve. It intersects the H axis at some value H_j. The line from point 1 to point a represents a characteristic having some concentration c_a, arising from the L curve. Its extension back to the H axis is a geometric construction. However, the entire line from H_j to a can be interpreted as a hypothetical characteristic that would have arisen from H_j if the initial concentration had been c_a. For such characteristics it was shown that correct concentration is given by:

$$c_a = c_0(H_0 - H_j)/(H_i - H_j) \tag{14}$$

And it can also be shown that:

$$S_a = c_0 H_0 / t_i \tag{15}$$

For characteristics not arising from the L curve, H_j becomes zero and Eq. 14 reduces to the standard Kynch form.

Given the relationship between concentration and free-settling flux S, a Kynch plot could be drawn for that part of the settling plot that is in free settling. By appropriate extrapolation it could be extended to synthesize or predict the S curve or Kynch plot above the compression point of the real batch test. Then G_{max} could be determined by a standard Yoshioka construction on the hypothetical or extended Kynch plot.

The suspension-sediment interface isn ot visible in a batch test. Measuring it as a function of time in a batch test requires sophisticated equipment and is not done in any accepted design procedure. As might be inferred by logical analysis from Figure 6B, the J-error decreases as the initial height of the settling column is increased. In an infinitely deep one, the L curve should approach linearity, and the J-error should approach zero. It seems probable that if the batch settling test is carried out in a deep column, the J-error may be small enough to disregard in view of all the other experimental uncertainties present.

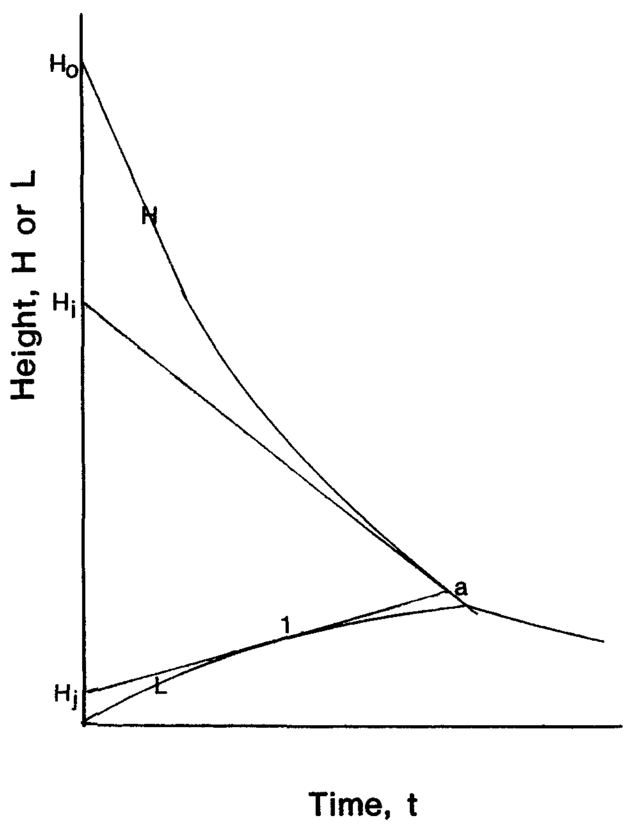

Figure 9. Construction to correct for J-error.

Validity of Mathematical Models

Mathematical models given in the literature assume that the Darcian permeability of a suspension is a function of concentration. In the free-settling range this means that the settling rate will be a function of concentration. The models then deduce mathematically how a system would behave if these assumptions were valid. Experimental data are not analyzed to validate the assumptions. In many, if not most, applications, the assumptions are not uniformly valid. Therefore, the mathematical theorists are deducing particle dynamics for systems that are, at least in part, merely hypothetical.

Short-Circuiting

Figure 10 shows a series of batch settling curves made at various initial concentrations C_0 on the same feed solids. At low initial concentrations, the curves appear much as would be predicted from flux theory. But above $C_0 = 485$, the settling plots curve downward until they reach what appears to be a compression point. In Figure 11, axes have been shifted so that the compression points for the various downward-curving plots coincide. As will be seen, the plots all come to the same

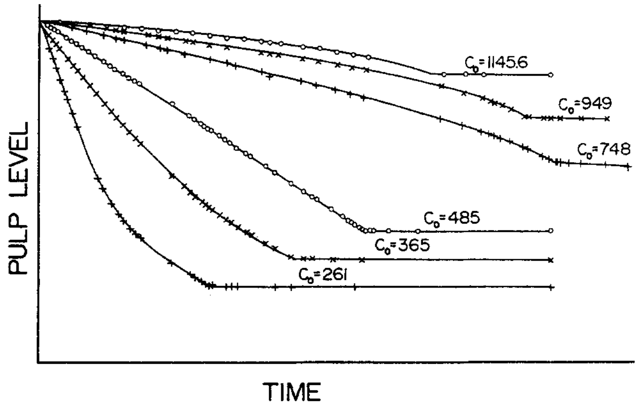

Figure 10. Settling plots for same suspension and initial height, but different initial concentrations.

subsidence rate as they approach their compression points. Samples pipetted from the top of the suspension after settling has proceeded for a time show concentrations below the original ones. (Fitch, 1966).

Such behavior is recognized in industrial practice as characteristic for flocculent suspensions and was reported by Michaels and Bolger (1962). It, however, is not what would be predicted on the basis of the models presented thus far. It is presumed to be the result of phase behavior. Apparently short-circuiting starts at some concentration (around 485 kg/m^3 in the example) and develops with time to produce an ever-increasing subsidence rate. When the subsidence rate at the top of short-circuiting zone becomes greater than the settling rate for some lower concentration, a zone of suspension at this critical lower concentration teeters or fluidizes off above the short-circuiting one.

One hypothesis to explain such behavior is given in Fitch (1966). It is deduced that where the Kynch plot has positive curvature (dS/dc positive), random local reverse gradients will propagate to reverse concentration discontinuities. Solids below the discontinuity would tend to settle away from solids above, leaving a parvoid. Such a concentration discontinuity is gravitationally unstable and would immediately upset if not inhibited by some global structure in the solids phase. In that case, the perturbation in concentration would be minor with little effect on the overall subsidence rate. However, if a solids structure formed above some critical concentration c_c inhibiting upset, the parvoids could grow to appreciable size. They would break through the superjacent structure in short-circuiting streams. Since local reverse gradients are conceived to be a random phenomenon, the number of parvoids formed and the amount of short-circuiting produced would be a function of time.

It would not affect thickener area demands if the suspension above c_c were in compression, provided that the augmentation of subsidence velocities were great enough to insure that no greater concentration would be limiting (Coe and Clevenger, 1916).

Under this hypothesis, one way to determine G_{max} would be to repeat tests like those illustrated in Figure 10. The critical concentration would be the one for which the settling plot was linear down to its compression point. However, although this strategy seems plausible, it has not been validated experimentally and must be considered no more than a working hypothesis at this time. Further, it requires a lot of testing. A procedure requiring only a single settling test would be desirable. The problem with this is to identify the critical concentration.

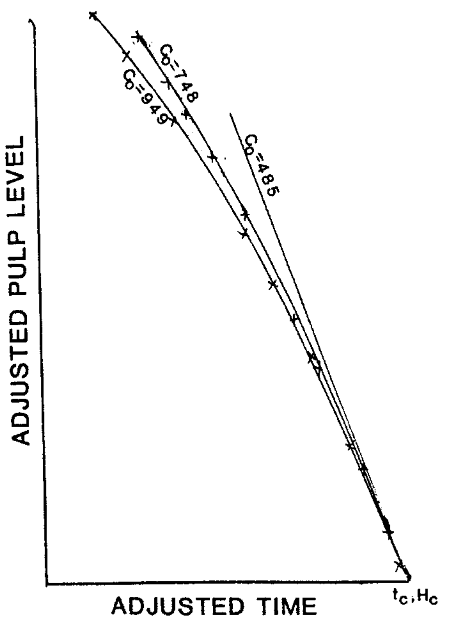

Figure 11. Height vs. time in vicinity of compression points.

Critical Concentration

An obvious manifestation of short-circuiting is channeling. There can be no question that it occurs. A channeled zone visibly develops in most batch thickening tests, and this has been reported in the literature by Dell and Kaynar (1968).

The channeled zone, at least with most of the calcium carbonate slurries studied, appears smooth, with no differential movement of individual floccules. Channels next to the cylinder wall seem to arise full-blown at or near the bottom of the zone, and maintain the same diameter to the top. Fluid streaming up the channels erupts from the top through craters in volcano-like mounds. These mounds persist and are visible over the entire surface after the suspension-supernatant interface falls to the top of the channeled zone. The fact that the mounds persist without slumping indicates that the solids structure in them has developed a yield value, and hence is in compression.

Suspension above the channeled zone appears fully fluidized. Individual floccules are perceptible and, just above the volcanos, move differentially. Jets of fluid from the volcanos persist for some distance, creating a visible and rapid upflow of entrained floccules and then rather abruptly disperse. Thus there is a zone of fluidized short-circuiting or "soft channeling" above the one of compression zone or "hard channeling." The top of the soft channeling zone is evidenced by rather abrupt appearance of "boils" at the pulp-supernatant interface when it falls to the top of the soft channeled zone.

Figure 12 shows an insert from a Tory plot for a deep column test made by the author. As will be apparent from the plot, subsidence rate of the suspension-sediment interface is strongly augmented following the appearance of "boils" at the interface. In such cases, the assumption that the critical concentration was reached at the time the boils appeared would seem reasonable. In strongly flocculating pulps such as those encountered in

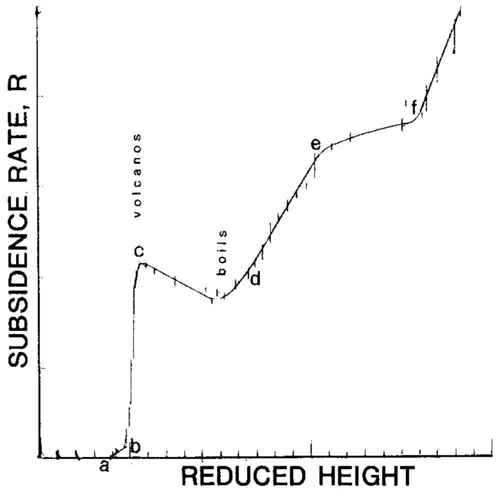

Figure 12. Tory plot for suspension showing strong short-circuiting.

metallurgical practice, this "dive into compression" is often great enough to be readily apparent in the batch test. There is a sudden and noticeable increase in subsidence rate just before compression is reached. In other suspensions, tle effect is not perceptible. It could be surmised or judged that short-circuiting is feeble in the latter case and that the critical concentration was at H_u.

Effect of Compression

It has been pointed out several times that G_{max} for a thickener is independent of solids compressibility.

A basic equation for compression thickening is (Fitch, 1966):

$$dx/dc = (dx/dc)^* \, [S/(S - G)] \qquad (16)$$

where $(dx/dc)^*$ is the inverse of the concentration gradient in a batch test after all settling is complete. Other equations have been deduced *de novo* in the literature. However, they start from the same premises, solve the same problem, and are alternative mathematical formulations for exactly the same physical relationships. They are mathematically equivalent to Eq. 16 and can be derived from it by appropriate substitution of variables. (For this not to be true there would have to be a mathematical error in one of the derivations.) The form given by Eq. 16 has the advantages of being directly related to Kynch and other flux theories, and makes a number of important relationships obvious. It is also a form which should be familiar to chemical engineers, since it is analogous to heat and material balances such as those for cooling towers (Dixon, 1979).

The term $S/(S - G)$ may be understood at a "stretch factor" showing how much greater a distance increment would have to be in a compressing sediment than it would be in a fully compressed bed.

Equation 16 shows directly that when S becomes equal to G at any concentration between that of feed and that of underflow, the stretch factor will become infinite and thus a critical zone will be formed. The Yoshioka construction shows geometrically where G becomes equal to S. Therefore, a Yoshioka diagram will determine the critical concentration and the limiting flux G_{max} in the case the critical zone lies in the compression regime just as it does for the case of free-settling (Fitch, 1966, 1979; Dixon, 1979). This is true because in a critical zone dc/dx is zero, and hence also the solids pressure gradient dPs/dx. In the absence of a pressure gradient, the actual settling rate u becomes equal to the free-settling rate u^*, and free-settling relationships are obtained. Therefore, G_{max} is completely independent of compression and floc compressibility.

It is also immediately apparent from Eq. 16 that compression depth will be minimum (not surprisingly) when G is zero. Therefore, a minimum or lower bound on compression depth necessary to yield an underflow concentration c_u would be:

$$\text{Min. Compression Depth} = \int_{c_0}^{c_u} (dx/dc)^*$$

In a Yoshioka diagram there are two cases to consider, Figure 13. The operating line, $G_t - c_u$, showing the values of G necessary to satisfy material balance, may intersect the flux curve at the feed or initial concentration c_0. In this case, the feed concentration is the critical one c_c. In the other case, the operating line $(G_t)' - (c_u)'$ becomes tangent to the flux curve at some concentration between c_0 and $(c_u)'$. In that case, the point of tangency marks the critical concentration. In either case, the limiting flux G_{max} could then be determined by the Coe and Clevenger equation:

$$G_{max} = u^*/(1/c_c - 1/c_u) \qquad (17)$$

However, in a Yoshioka diagram G_{max} can be read directly from the intercept of the operating line with the flux axis.

Pure theoreticians much prefer algebraic representations of physical relationships over geometric representations such as Yoshioka diagrams. The Yoshioka diagram is easily reduced to algebraic form by a simple exercise of analytical geometry. For the tangent case, c_c can be determined by solving the equation:

$$dS/dc = -S/(c_u - c) \qquad (18)$$

Thus if free-settling rate u^* can be represented as a power function of c over the range of interest, i.e., $u^* = Mc^n$, then

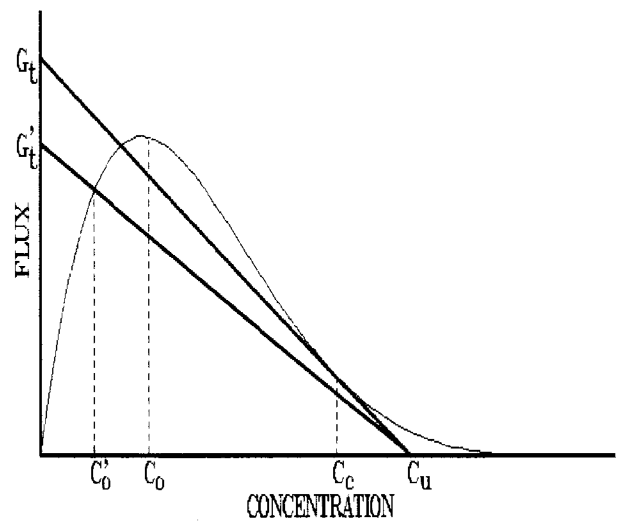

Figure 13. Yoshioka diagram showing different operation lines.

solution of Eq. 17 yields:

$$c_c = c_u(n + 1)/n \tag{19}$$

G_{max} can be found by substitution of c_c in Eq. 17.

Notation

A = area normal to direction of settling
A_{ch} = area covered by characteristic in steady-state thickening
c = reduced concentration–volume fraction solids
c_0 = initial concentration
c_c = critical concentration
c_u = underflow concentration
g = acceleration of gravity
G = settling flux
G_{max} = maximum thickener flux
G_t = total flux past a level in continuous thickening
H = height
H_0 = initial height in batch test
H_b = depth of sedimentation basin
H_i = height of Kynch intercept
H_j = height of L curve tangent intercept
H_u = underflow height = c_0H_0/c_u
K = standard Darcy permeability constant
L = height of sediment-suspension interface in a batch test
P_L = dynamic liquid pressure
P_s = solids pressure
Q = solids flow
R = subsidence rate of suspension-supernatant interface
S = free-settling flux, cu^*
t = time
u = velocity of solids
u^* = settling rate in the absence of pressure gradient, solids velocity relative to a system in which total flux (liquid + solids) = 0
v_K = propagation velocity of Kynch characteristic
v_u = velocity of system due to underflow withdrawal
W = basin width
μ = liquid viscosity
ρ_l = liquid density
ρ_s = solids density
ϕ = darcy flux

Literature Cited

Coe, H. S., and G. H. Clevenger, "Method for Determining Capacities of Slime-settling Tanks," *Trans. AIME*, **55**, 356 (1916).

Dell, C. C., and M. B. Kaynar, "Channeling in Flocculated Suspensions," *Filtration and Separation*, p. 323 (July/Aug. 1968).

Dixon, D. C., "Theory of Gravity Thickening," *Progress in Filtration and Separation, Vol. 1*, Elsevier (1979).

Fitch, B., "Computer Programs SEDANAL (Sedimentation Analysis) and THICKNER (Thickener Design)," available on diskettes *Fluid/Particle Separ. J.*, Amer. Filtration Soc., available on diskettes (1990).

———, "Current Theory and Thickener Design," *Ind. & Ind. Chem.*, **58**, 18 (Oct., 1966).

———, "Flow Path Effect on Sedimentation," *Sewage & Ind. Wastes*, **28**, 1 (1956).

———, "Kynch Theory and Compression Zones," *AIChE J.*, **29**, 940 (1983).

———, "A Mechanism of Sedimentation," *I. & E.C. Fund.*, **5**, 129 (Feb., 1966).

———, "Sedimentation of Flocculent Suspensions, State of the Art," *AIChE J.*, **25**, 913 (1979).

———, "Unresolved Problems in Thickener Design and Theory," *Research Conf., Filtration and Separation*, Soc. of Chem. Engrs., Japan (1972).

Hazen, A., "On Sedimentation," *ASCE Trans.*, **33**, 45 (1904).

Talmage, W. P., and E. B. Fitch, "Determining Thickener Unit Areas," *I. & E.C.*, **47**, 38 (1955).

Tory, E. M., "Batch and Continuous Thickening of Slurries," PhD Thesis, Purdue Univ. (1961).

Turner, J. P. S., and D. Glasser, "Continuous Thickening in a Pilot Plant," *I. & E.C. Fund.*, **15**, 23 (1976).

Yoshioka, N., Y Hotta, S Tanaka, S. Naito, and S. Tsugami, "Continuous Thickening of Flocculated Homogeneous Slurries," *Kagaku Kogaku*, **21**, 66 (1957).

Manuscript received Jan. 24, 1990, and revision received Aug. 9, 1990.